Acta Zoologica (Stockholm) **81**: 93–107 (April 2000)

Microstructure variation in sponges sharing growth form: the encrusting demosponges *Dysidea avara* and *Crambe crambe*

Jordi Galera[1], Xavier Turon[1], María J. Uriz[2] and Mikel A. Becerro[2]

[1]Department of Animal Biology (Invertebrates) Faculty of Biology University of Barcelona 645, Diagonal Ave E-08028 Barcelona Spain
[2]Centre for Advanced Studies (CSIC) Camí de Sta. Barbara s/n E-17300 Blanes, Girona Spain

Keywords:
microstructure, cytology, ecological strategy, growth form, sponges

Accepted for publication:
29 November 1999

Abstract

Galera, J., Turon, X., Uriz, M. J. and Becerro, M. A. 2000. Microstructure variation in sponges sharing growth form: the encrusting demosponges *Dysidea avara* and *Crambe crambe*. — *Acta Zoologica* (Stockholm) **81**: 93–107

The goals of this study are to assess variability of microarchitecture in sponges with a similar growth form and to look for correlates between microstructural organization, biological functions and ecological strategies. A comparison of the microstructure of the encrusting sponges *Dysidea avara* (Dendroceratida) and *Crambe crambe* (Poecilosclerida) is performed. The species co-occur in sublittoral habitats of the western Mediterranean. Histological techniques, image analysis and corrosion castings are used in order to quantify thickness, degree of development of the aquiferous system, relative amount of structural and cellular materials, and size of the choanocyte chambers in both species. The fine structure and cellular types are described and analysed through SEM/TEM. These sponges are known to feature contrasting ecological strategies: *D. avara* has higher growth and clearance rates than *C. crambe*, it is more susceptible to predation and uses a more opportunistic strategy of space acquisition and maintenance. *C. crambe* grows slowly, it is chemically protected from predation and it competes successfully for space with other invertebrates. These differences in biological strategies are here shown to have clear structural correlates: *D. avara* is structurally simpler, with fewer cell types and very scarce matrix material. Most of its section is occupied by the highly developed aquiferous system. Its construction is much looser than in *C. crambe*. In the latter species, structural complexity is higher, it produces long-lasting structures such as the spicules, and it is more compact and thinner. It is concluded that there is wide scope for microarchitectural patterns, even in species with similar growth form, and that structural and cytological characters may prove to be useful descriptors of biological strategies in sponges.

Xavier Turon, Department of Animal Biology (Invertebrates), Faculty of Biology, University of Barcelona, 645 Diagonal Ave., E-08028 Barcelona, Spain. E-mail: xaviert@bio.ub.es

Introduction

Growth form has been suggested as a major correlate of biological characteristics and space occupation strategy in benthic modular animals (Buss 1979; Jackson 1979). Encrusting forms are surface-dependent and therefore their fitness could rely on some efficient mechanism for space acquisition and maintenance. In this paper, we analyse the cytology and microstructure of two co-occurring encrusting sponges: the poecilosclerid *Crambe crambe* (Schmidt, 1862) and the dictyoceratid *Dysidea avara* (Schmidt, 1862).

C. crambe is a well-known sponge from the points of view of its biology, ecology and chemical defence (Uriz *et al.* 1996a; Becerro *et al.* 1997; Turon *et al.* 1998). On the other hand, data on the biological features of *D. avara* are accumulating (Uriz *et al.* 1996b,c; Turon *et al.* 1997). In addition, the

chemistry of *Dysidea* species has been well documented (Minale *et al*. 1974; Müller *et al*. 1985; Sica *et al*. 1987; Crispino *et al*. 1989; De Giulio *et al*. 1990). The previous studies on the two species have revealed contrasting ecological strategies: *D. avara* has higher growth and clearance rates than *C. crambe*, it is more susceptible to predation (despite potentially defensive compounds such as avarol, Uriz *et al*. 1996b) and uses a more opportunistic strategy of space acquisition and maintenance. *C. crambe* is a slow-growing form, it is chemically protected from predation and it competes successfully for space with other invertebrates.

Sponges are relatively simple Metazoans that lack true tissues and whose biological functions are accomplished mostly at a cellular level (Simpson 1984). For instance, a more developed aquiferous system can imply higher food capture efficiency and hence higher potential growth rates, a higher amount of structural material (collagen, spicules) may render the species less susceptible to predation, and so on. These features make sponges particularly suited to test the hypothesis that microarchitectural patterns reflect the ecological strategies of sponges. The goal of this paper is to demonstrate the potentially informative properties of structural and cytological parameters as descriptors of biological strategies by comparing two sympatric sponges with similar shapes that have contrasting ecological features.

Materials and Methods

D. avara is a whitish-violet sponge that covers moderately shaded substrata in the sublittoral zone in the western Mediterranean. Its morphology is usually encrusting in shallow habitats (down to 20 m in depth), although it changes to massive or even erect in some deeper habitats and on the bottom of caves. Its surface is free of macro-epibionts, except for some seasonal red algae. *C. crambe* is a red encrusting sponge which dwells on both well-illuminated and relatively shaded habitats, and is always free of both macro- and microepibionts (Becerro *et al*. 1997). *D. avara* (of encrusting morphology) and *C. crambe* specimens were collected at depths of between 10 and 20 m by SCUBA diving at the localities of Blanes and Tossa de Mar (NE of Spain, western Mediterranean), during the years 1993–96. Potential geographical variation in microstructure of the species is beyond the scope of this paper, as specimens were collected in the same region of the western Mediterranean. Small pieces of the sponges, 4–6 cm^2 in surface area, were cut underwater, transported to the laboratory in seawater and fixed in different ways according to the diverse methodologies used.

Histology and microscopy methods

For light microscope studies, the material was fixed in 4% formalin, decalcified with a 19 : 1 mixture of 4% formalin and pure nitric acid for 2 h and desilificied with 5% hydrofluoric acid (HF) for 2 h, in order to dissolve both foreign material inside the fibres in *D. avara* and siliceous spicules in *C. crambe*. Samples were afterwards dehydrated in an ethanol series, embedded in paraffin and sectioned (5–8 μm thick) perpendicularly to the sponge's surface. We assume that the possible effects (e.g. shrinking) of the manipulations (dehydration, desilicification) will affect both species equally, so that comparative analysis are not hindered by differential alterations.

The histological sections were stained with haematoxilin-eosin for general observation of both species. For parameter quantification, we used Mallory's stain for *C. crambe* and Diff-Quick for *D. avara*. Staining followed standard procedures (Martoja and Martoja 1970). The Mallory procedure stains the nuclei in red, spongin and collagenous fibrils in blue and cytoplasmatic granules in orange-red. Diff-Quick stains cells in pink and spongin fibres and collagen in intense blue. In *C. crambe*, the Mallory trichromic stain offered a clear differentiation of the diverse elements, but the same method was not resolutive in *D. avara*, for which the Diff-Quick stain gave more satisfactory results.

For transmission electron microscopy (TEM), fixation was carried out for 5 h in 2.5% glutaraldehyde in 0.1 M cacodylate buffer (osmolarity adjusted to 980 mOsm with sacarose) and the materials were post-fixed for 90 min with OsO_4 (1%) in the same buffer. Some samples were also desilicified for 2 h. in 0.5% hydrofluoric acid in the same buffer. Between each step the material was washed three times with buffer, for 10 min each. The samples were then dehydrated in an acetone series and embedded in Spurr's resin. Ultrathin sections were stained with uranyl acetate and lead citrate and examined with a Hitachi H-600 transmission electron microscope belonging to the Microscopy Unit of the Scientific and Technical Services of the University of Barcelona.

For scanning electron microscopy (SEM), samples were fixed in a 6 : 1 mixture of 2% osmium tetroxide (OsO_4) in seawater and saturated mercury chloride ($HgCl_2$) in distilled water for 90 min (Johnson and Hildemann 1982). The sponges were then frozen in liquid nitrogen and freeze-fractured. They were critical-point dried, mounted and sputter-coated with gold following standard procedures and examined through a Hitachi-2300 scanning electron microscope (Microscopy Unit, University of Barcelona).

Image analysis

For the quantification of the different components of the sponge, histological sections were digitized using a video-camera incorporated in a light microscope and studied by image analysis (IMAT software, developed by the University of Barcelona). Two magnifications were used for general observation (magnification 40×; $n = 10$ and $n = 24$

specimens for *D. avara* and *C. crambe*, respectively) and detailed observation (magnification 200× for *D. avara* and 400× for *C. crambe*; $n = 14$ and $n = 24$ specimens, respectively). Due to the differential staining, the program was able to discern and quantify the areas that corresponded to cells, spongin, diffuse collagen and matrix (ground substance of the mesohyl). General images at low magnification were used to quantify porosity (empty spaces corresponding to canals and chambers of the aquiferous system) and spongin. Images at high magnification were used to quantify cells, collagen fibrils and matrix in both choanosome and ectosome. The values obtained for choanosome and ectosome were treated separately or combined (in proportion to the relative thickness of both layers) to obtain a global value. Three images (i.e. replicates) at each magnification were captured from separate slides of each sponge specimen. All relevant parameters are expressed as ratios between the component being quantified and (a) the total area of the sponge section and (b) the total area discounting the aquiferous system area (i.e. area of canals and chambers). In addition, other parameters such as ectosome and choanosome thickness and diameter of inhalant pores were measured directly on the slides with the help of a calibrated eyepiece. Area of the choanocyte chambers was also measured in the slides by taking the major and minor axes of haphazardly chosen chambers (between 5 and 10 chambers from different slides of each specimen, 10 specimens per species) and then applying the formula for the area of an ellipse.

The quantitative parameters were statistically analysed using a nested analysis of variance, with species as the main factor (fixed) and specimen as the nested factor (random). The replicates were the three slides measured per specimen or, in the case of the choanocyte chambers, the chambers measured for each specimen. The nested ANOVA allowed us to test the effect of the species once the variance associated with the sponge individuals has been partialled out. The data were log-transformed to meet the assumptions of parametric techniques and analysed using the Systat v5.0 package. The mean and standard error values given in text and graphs are obtained by using a single value per specimen (averaging any within specimen replicate).

Corrosion casts

We also obtained resin castings of the aquiferous systems of both species with the techniques described in Bavestrello *et al.* (1988), Burlando *et al.* (1990) and Rosell (1996). The castings were prepared with Batson's 17 Plastic Replica and Corrosion Kit (Polysciences Inc., Warrington), with the different components mixed in the proportions recommended by the manufacturer. The final polymer was injected with a glass syringe through the oscula of both species. Two different procedures were tested: (a) the specimens were collected underwater and transported to the laboratory, where they were allowed to expand for some hours in aerated aquaria before injection, and (b) the two solutions were taken separately and mixed underwater, and sponge specimens were injected *in situ* and collected after one hour with the help of a hammer and chisel. The plastic was in both cases allowed to polymerize for 24 h and the samples were afterwards treated with 5% sodium hypochlorite for some days until complete elimination of the organic matter. Finally, the casts were rinsed with distilled water, lyophilized, covered with gold (sputtering method) and observed under SEM.

Results

General structure

In all statistical analyses, the specimen (nested) factor proved significant, indicating a marked intraspecific variability. We will only indicate therefore the statistical significance of the factor species obtained in the nested ANOVAs. Values are always given as mean ± standard error.

The surfaces of *D. avara* present conules, which are elevations corresponding to the tips of the primary fibres and where a network of ectosomal thickenings or ribs converges. Between these conules lie the inhalant pores or ostia (30.8 ± 2.2 μm in diameter). *C. crambe* presents a smooth, nonconulous surface from which the excurrent canals protrude. The ostia in the latter species (11.4 ± 1.2 μm) are significantly smaller than in *D. avara* ($P < 0.001$, nested ANOVA).

The general aspect of the sponge sections of both species and of the resin castings of the aquiferous systems is shown in Figs 1–6. The sponge organization features a distal layer, or ectosome, and a basal layer, or choanosome. A zone of wide canals separates both layers, which often show a distinct staining due to their diverse composition (see below).

In spite of the encrusting shape of both sponges, differences in structure are readily evident (Figs 1–4). Mean thickness is significantly ($P < 0.001$) higher in *D. avara* (3629 ± 260 μm) than in *C. crambe* (1064 ± 88 μm) (Fig. 7). Ectosome mean thickness is not significantly different ($P = 0.175$) in the two species: 295 ± 25 μm for *D. avara* and 376 ± 38 μm for *C. crambe*. The different thickness is therefore due to the much thicker choanosome of *D. avara* (3335 ± 257 μm) as compared to that of *C. crambe* (689 ± 71 μm, $P < 0.0001$). The ratio between choanosome and ectosome is accordingly much higher in *D. avara* (about 12 times thicker the choanosome than the ectosome) than in *C. crambe* (just about double the choanosome than the ectosome) (Fig. 7).

Another clear structural difference between the two species is the degree of porosity (i.e. the ratio between the surface area of canals and chambers relative to the total sponge surface in the slides). As defined here, porosity is equivalent to the relative amount (in area) of the aquiferous system per sponge section. Porosity is significantly

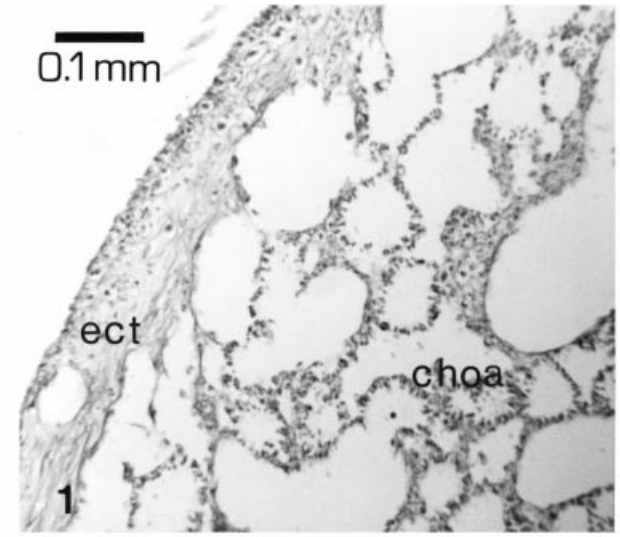

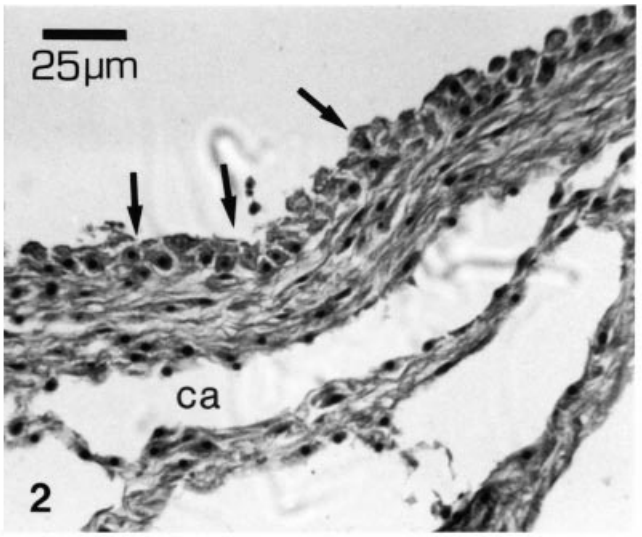

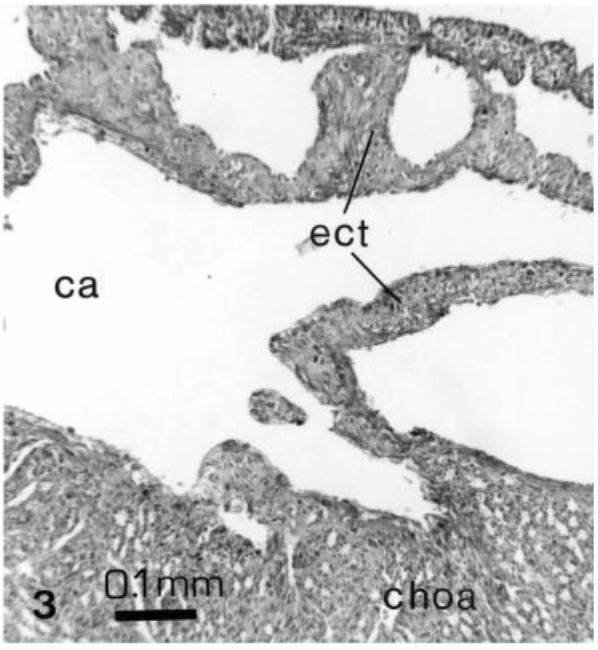

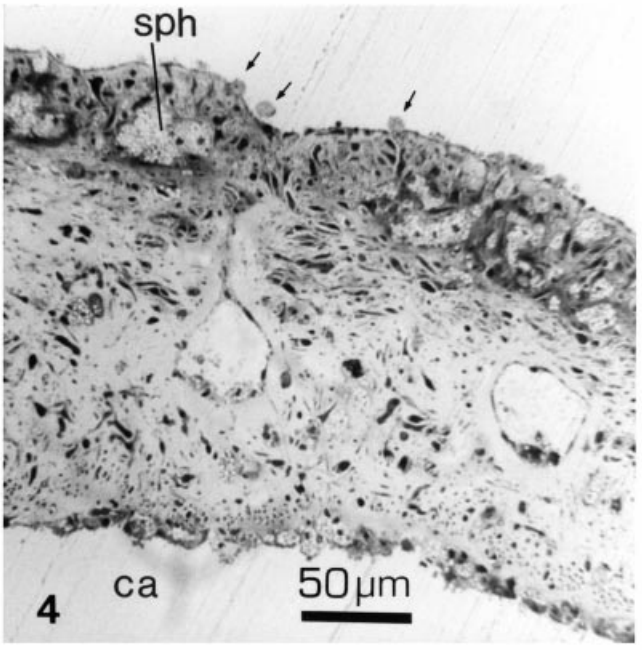

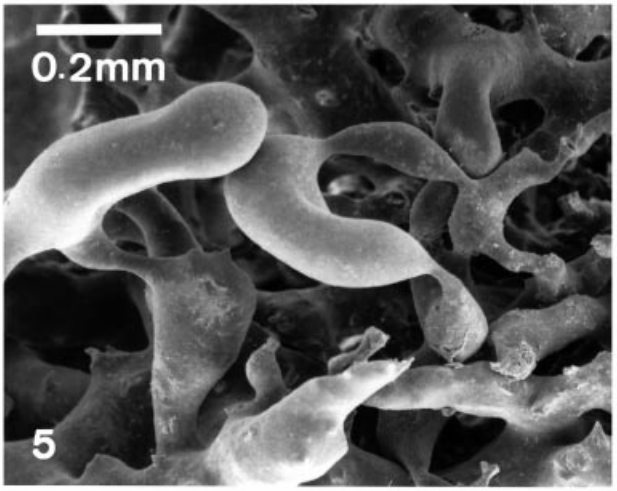

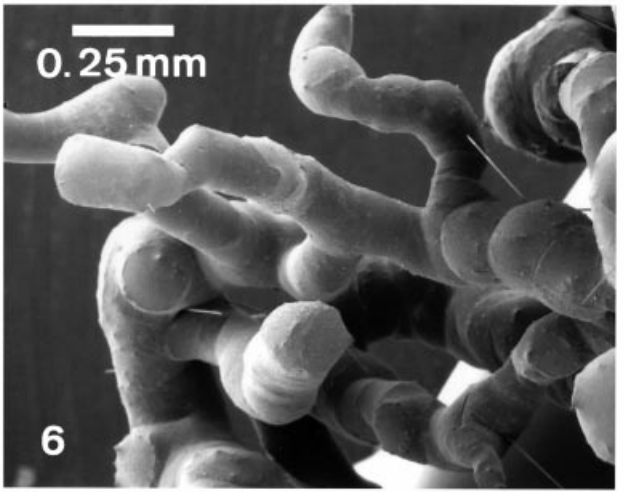

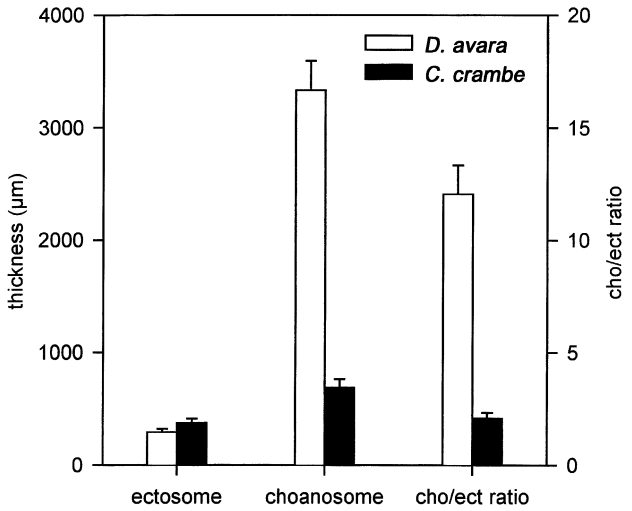

Fig. 7—Thickness of the sponge layers and choanosome/ectosome ratio in the species studied. Bars are standard errors.

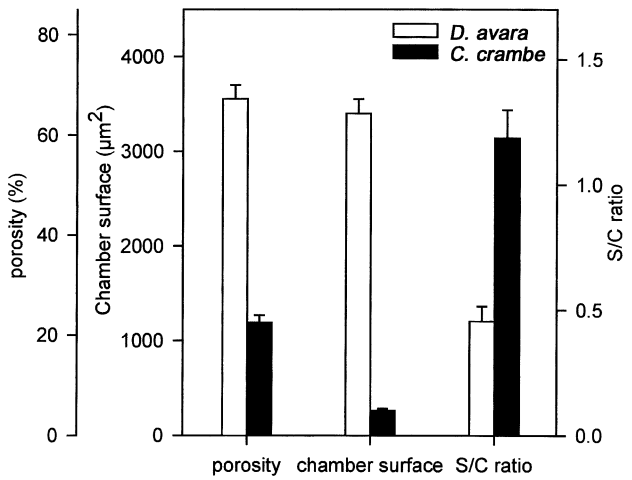

Fig. 8—Values of porosity, surface of chambers and ratio between structural and cellular material (S/C ratio) in the species studied. Bars are standard errors.

($P < 0.001$) greater in *D. avara* ($67.2 \pm 0.03\%$ of the section area corresponds to canals and chambers) than in *C. crambe* ($22.5 \pm 0.01\%$). Thus, although *D. avara* is about three times thicker than *C. crambe*, it is also three times more porous (Fig. 8). The surface of the choanocyte chambers measured in sponge sections is also significantly greater

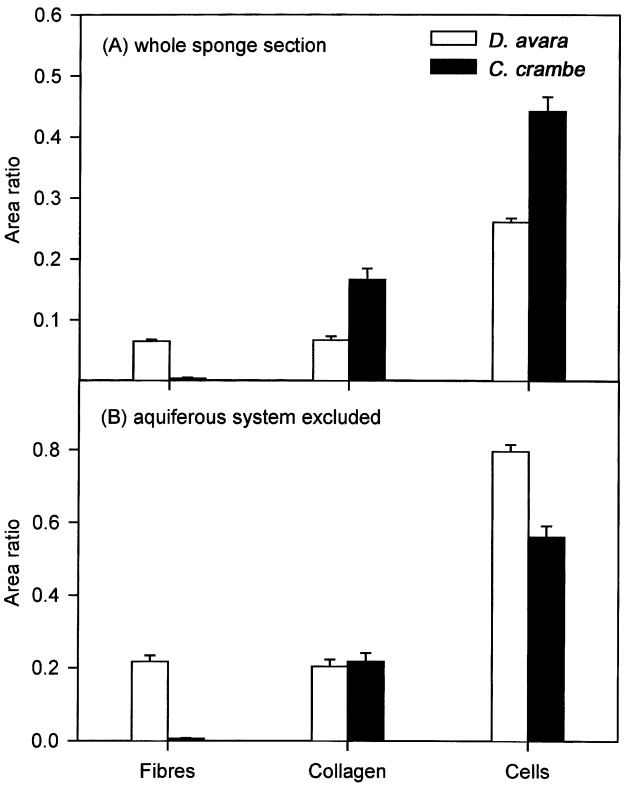

Fig. 9—Amount of fibres, collagen, and cells in the species studied, relative to (**A**) the whole sponge section or (**B**) the sponge section minus the aquiferous system surface area. Bars are standard errors.

($P < 0.001$) in *D. avara* (3404 ± 473 µm^2) than in *C. crambe* (261 ± 21 µm^2) (Fig. 8).

There are also differences in the main structural components of the sponges: spongin fibres, intercellular collagen, and cells (Fig. 9a). Here we will call 'fibre' both the perispicular spongin of *C. crambe*, which surrounds spicules, and the typical spongin fibres of *D. avara*. The amount of fibres (as measured by the surface area of fibres relative to total sponge surface area) is significantly higher ($P < 0.001$) in *D. avara* (0.065 ± 0.002) than in *C. crambe* (0.004 ± 0.001). In contrast, there are significantly less intercellular collagen fibrils in *D. avara* (0.067 ± 0.006, area ratio, for 0.167 ± 0.02 in *C. crambe*, $P < 0.001$), and also less cellular material per section (*D. avara*, 0.261 ± 0.006; *C. crambe*, 0.442 ± 0.024, $P < 0.001$). However, the different porosity of both species can make these comparisons misleading if referred to total

Fig. 1—*Dysidea avara*, histological section through the ectosome (ect) and the upper part of the choanosome (choa).
Fig. 2—*Dysidea avara*, enlarged view of the ectosome region. Arrows point to exopinacocytes (ca canal).
Fig. 3—*Crambe crambe*, histological section through the ectosome (ect) and the upper part of the choanosome (choa) (ca canal).
Fig. 4—*Crambe crambe*, enlarged view of the ectosome. Arrows point to cells leaving the sponge surface (ca canal, sph spherulous cells).
Fig. 5—*Dysidea avara*, SEM image of a corrosion casting of the aquiferous system.
Fig. 6—*Crambe crambe*, SEM image of a corrosion casting of the aquiferous system.

sponge section. The same parameters referred to the actual surface occupied by sponge material (excluding the canals and chambers of the aquiferous systems) reveals a different pattern (Fig. 9b). The difference in the amount of fibres is even more marked (*D. avara*, 0.217 ± 0.017; *C. crambe*, 0.006 ± 0.001, $P < 0.001$), but the differences are no longer significant as regards collagen material (*D. avara*, 0.204 ± 0.019; *C. crambe*, 0.218 ± 0.024, $P = 0.361$), and the relationship is reversed for the amount of cellular material, now higher in *D. avara* (0.796 ± 0.019), than in *C. crambe* (0.561 ± 0.030, $P < 0.001$).

Another parameter appears clearly distinct between species. In *C. crambe* there is a noticeable amount of matrix. We designate as matrix the ground substance of the mesohyl, that is, the sponge surface not occupied by fibres, collagenous fibrils, or cells. This matrix is almost lacking in *D. avara*, while it occupies 0.286 ± 0.019 of the sponge sections (0.370 ± 0.023 excluding the aquiferous system) in *C. crambe*. We can obtain an estimate of the relative investment in structural and cellular elements by calculating the ratio between noncellular elements (fibres, collagen, and matrix) and cells in both species. We will call this ratio the structural-cellular material (S/C) ratio. The structural elements are significantly ($P < 0.001$) more important in *C. crambe* (S/C ratio: 1.188 ± 0.111) than in *D. avara* (S/C ratio: 0.455 ± 0.059, Fig. 8).

The corrosion castings highlight the differences in structure of the aquiferous system in these species. It should be noted that the castings provide information about the exhalant part of the canal system, as the plastic was introduced through the oscula. The finer branches of the castings end in apopyles and choanocyte chambers. We only have therefore a tri-dimensional image of the exhalant system with this method. In *D. avara*, the castings show a finely branched, anastomosed mesh of canals occupying most of the casting volume (Fig. 5), while for *C. crambe*, the exhalant system featured a pattern of thick and coarsely branched canals which filled the space only partially (Fig. 6), a fact consistent with the lower porosity and higher matrix content of this species.

Apart from porosity and fibres, which were quantified on low magnification images, the remaining parameters were obtained separately from the ectosome and the choanosome of the sponges and then combined (in proportion to the relative thickness of the two layers). In Fig. 10, however, these values (as surface ratios relative to total surface excluding the aquiferous system) are presented separately for both layers. Intercellular collagen is in both species more abundant in the ectosome, while the reverse is true for the cellular components, the differences between layers being significant for both variables in both species (paired-sample *t*-test analyses on the average values per specimen, all $P < 0.001$). *D. avara* has significantly more collagen than *C. crambe* in both the choanosome and the ectosome layers (nested ANOVAs, $P < 0.001$). Note, however, that the very different ratio between ectosome and choanosome in these species balances the values of collagen when both layers are combined (Fig. 9b). *D. avara* also has more cellular material in both ectosome ($P = 0.026$) and choanosome ($P < 0.001$). On the contrary, while matrix material is negligible in *D. avara*, it accounts for 0.274 ± 0.026 of the sponge material (excluding the aquiferous system) in the ectosome of *C. crambe*, and 0.340 ± 0.027 in the choanosome. The between-layer difference in this parameter is not significant (paired *t*-test, $P = 0.102$).

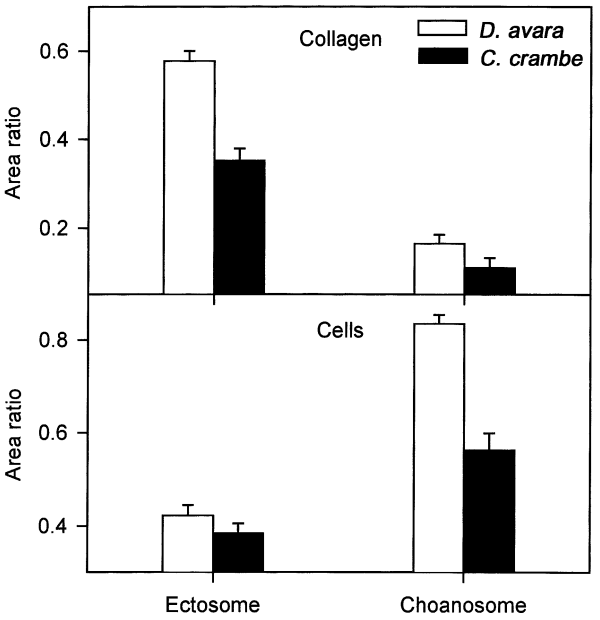

Fig. 10—Relative amount of collagen and cells in the ectosome and the choanosome of the species studied (aquiferous system excluded for the surface area calculations). Bars are standard errors.

Figs 11–16—*Dysidea avara*. c collagen, ca canal, cch choanocyte chamber, ch choanocyte, exp exopinacoderm, f flagellum, mh mesohyl, pi pinacocyte, v secretion vesicle.

Fig. 11—SEM image of the ectosome (freeze-fracture). Arrows indicate collencytes.

Fig. 12—Detail of the collagen fibrils.

Fig. 13—Section of an endopinacocyte lining a canal. Several vesicles extrude their contents to the canal's lumen (asterisks).

Fig. 14—SEM image of the endopinacoytes lining the exhalant canals of the aquiferous system, with a single flagellum each. Note the extrusion of vesicles, corresponding to those seen in Fig. 13.

Fig. 15—Image of a collencyte filled with secretion vesicles and producing a strand of collagen fibrils.

Fig. 16—SEM image (freeze-fracture) of the choanosome, showing a choanocyte chamber (lower left) and a canal (upper right). Note the poorly developed mesohyl between the two.

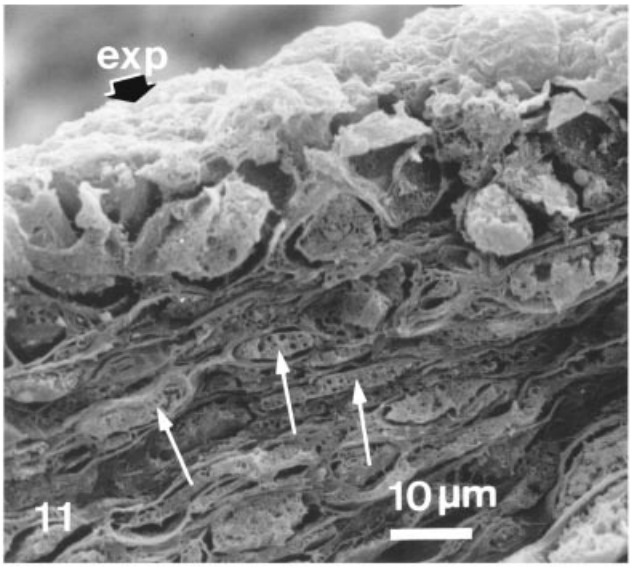

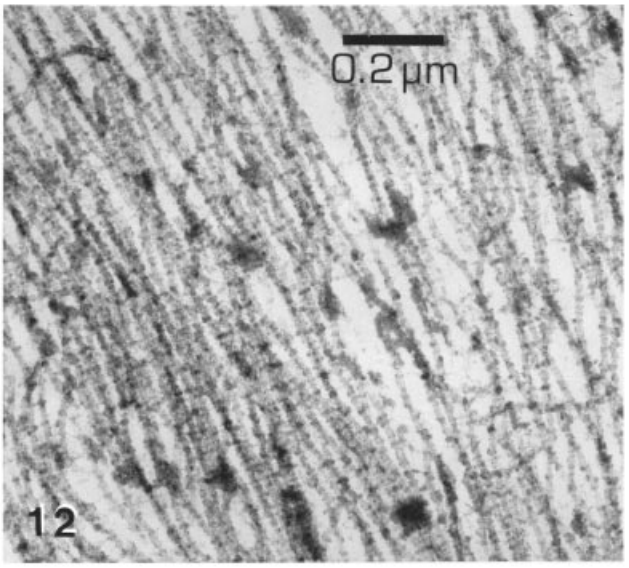

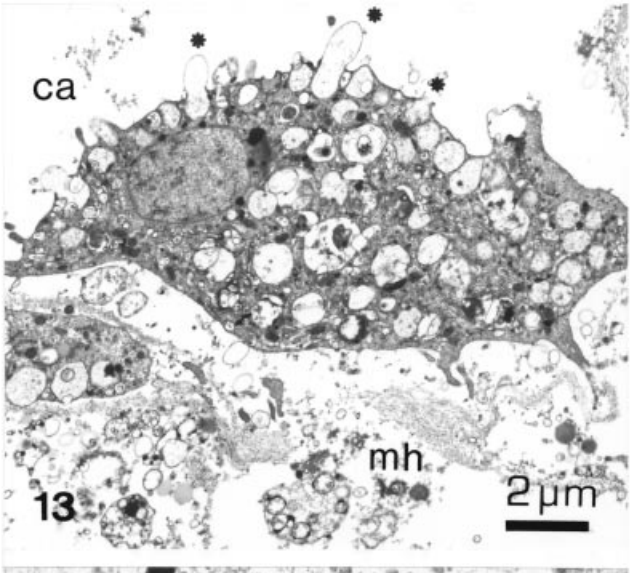

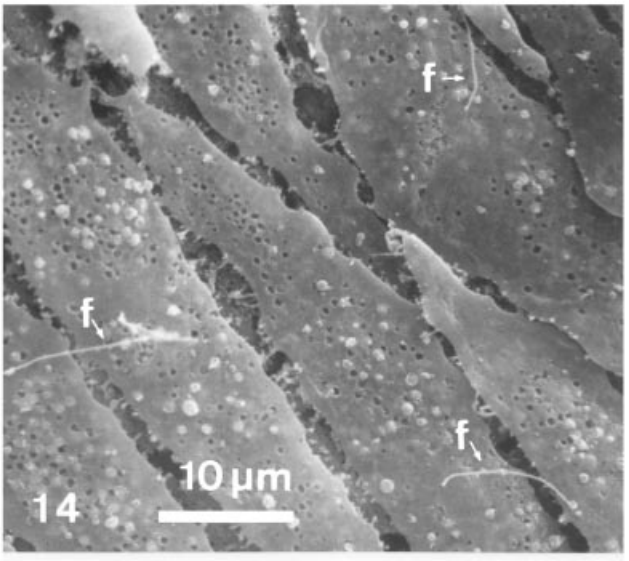

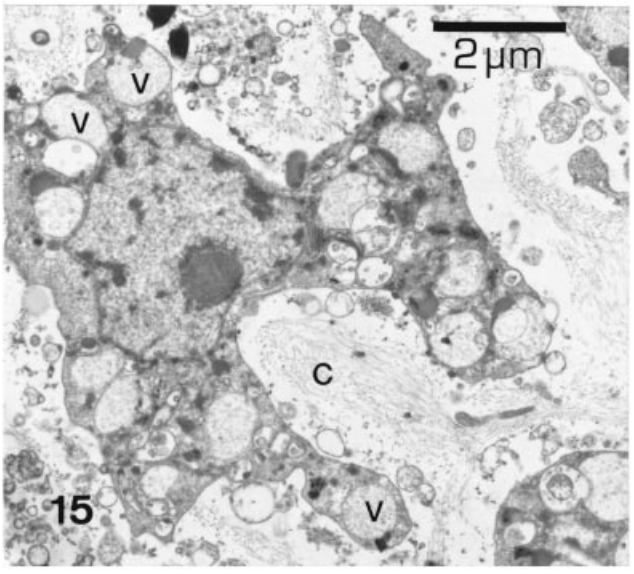

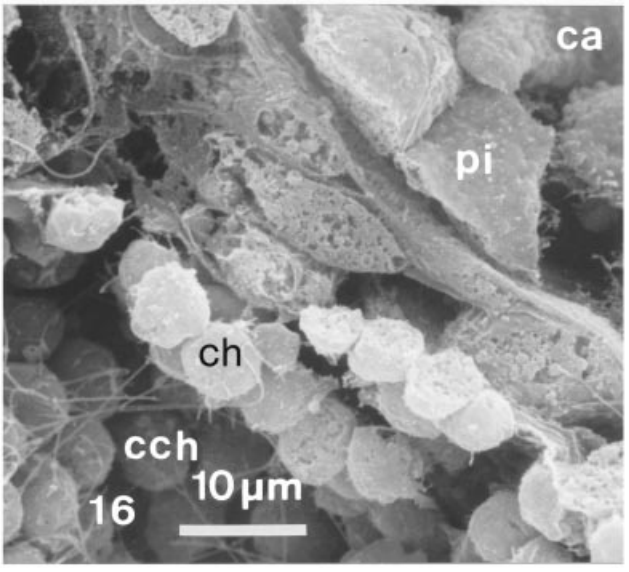

Fine structure and cytology

Dysidea avara. A layer of exopinacoderm covers the outer surface of the sponge. Below it there is a zone occupied mostly by elongated collencytes where abundant collagen fibrils appear packed around the cells (Fig. 11). The fibrilar collagen corresponds to the intercellular type called spongin A by Gross *et al.* (1956) and it is morphologically rough, as described in Garrone (1985). Collagen fibrils have an average diameter of about 200 Å and feature a transverse banding at approximately 430 Å intervals (Fig. 12). Endopinacocytes are also present within the ectosome of *D. avara*, lining the canals of the aquiferous system. These endopinacocytes (Fig. 13) measure up to 23 μm in length and up to 8 μm in thickness and often display thin lateral processes. One main feature of the pinacocytes is that their cytoplasm is usually packed with vesicles of clear contents that appear to be continuously shed to the canals' lumen (see Figs 13 and 14). The endopinacocytes lining the excurrent canals possess a short flagellum (Fig. 14), 9–11 μm in length. This feature is characteristic of some sponge Orders: Homosclerophorida, Dictyoceratida, Dendroceratida and Haplosclerida (De Vos *et al.* 1991).

The collencytes are the most abundant cell type in the ectosome. They are 9–13 μm in diameter (Fig. 15). This cell-type is amebocyte-like in shape, with cytoplasmatic expansions intermingled with the collagen fibrils. The large nuclei of these cells (about 3.5 μm in diameter) are nucleolate. They possess a finely granulated cytoplasm with inclusions and phagosomes. Their main diagnostic feature is the large vesicles, 0.5–1 μm in diameter, that presumably contain the collagen precursors.

There is practically no ground substance between the cells in the choanosome of *D. avara* (Fig. 16). Choanocytes and pinacocytes are the main cellular types in the choanosome, although archeocytes and collencytes are also present. The choanosome structure is formed by large, elongated flagellated chambers reaching 90 μm in diameter (mean of 60 μm through electron microscopy). Measures obtained with corrosion castings are slightly bigger (mean of about 94.5 μm) (Fig. 17). The apopyles, as measured in the castings, were 21.8 μm in diameter.

The number of choanocytes (subspherical or elongated in shape, 9–13 μm in largest diameter) per chamber is variable, ranging from 20 to 40 in a given section. The choanocytes are peculiar in not having the nuclei in a basal position, but distally placed as in Calcaronea sponges (Figs 18, 19). Between the nucleus and the flagellum there is always a well-developed Golgi complex, associated to the flagellum basis. The nuclei display chromatin grains and a conspicuous nucleolus, typical in highly active cells. The size of the nuclei ranges between 2 and 5 μm in diameter. The cytoplasm of these cells is packed with inclusions, giving the cells a granular and 'spherulous' appearance. Three main types of vesicles can be distinguished under the electron microscope: phagosomes, and small and large inclusions (Fig. 19). Phagosomes appear near the bases of the flagella, and consist of vacuoles of heterogeneous contents. Their function is clearly digestive and their size range is very variable. The second type consists of electron-dense secretions about 0.2 μm in size, often in close association with the Golgi complex, while the third type are larger inclusions (about 1 μm) of moderately electron-dense material.

The choana, about 4 μm in diameter, are formed by ≈ 40 microvilli in average, each with a mean diameter of 0.1 μm (0.075–0.15). The gap between microvilli is 0.17 ± 0.06 μm wide (Fig. 20).

The archeocytes of *D. avara* have ovoid or elongated morphology (up to 20 μm in length) with a large (up to 5 μm in diameter), nucleolate nucleus, some glycogen reserves and a variable number of phagosomes and vesicles (Fig. 21). They are relatively abundant in the choanosome, sometimes displaying complicated pseudopodia.

D. avara lacks a mineral skeleton, although the spongin fibres usually contain foreign material (sand grains, shell and spicule debris) and form a network providing skeletal support (Fig. 22). Degeneration areas can be found very close to other functional zones of the same specimen. In the degenerating areas, a mixture of vesicles, membranes and nuclei appear free within the mesohyl's ground substance. These degeneration areas may be the result of the continuous process of disintegration and reorganization of the sponge structure described for other species (Diaz 1979).

Crambe crambe. The ectosome of *C. crambe* is formed by exopinacocytes, endopinacocytes, collencytes, spherulous cells and a collagen-rich mesohyl. The endopinacocytes are flat and triangular in section. They have thin, long lateral processes. With the latter included, the pinacocytes

Figs 17–22—*Dysidea avara*. cho choana, exp exopinacoderm, f flagellum, *n* nucleus, nu nucleolus, lv large vesicle, sv small vesicle, ph phagosome.

Fig. 17—SEM detail of a corrosion casting corresponding to the finer part of the aquiferous system. Some choanocyte chambers are indicated by arrows.

Fig. 18—SEM image of a group of choanocytes. The one on the right is freeze-fractured and shows the nucleus (*n*) and some phagosomes (asterisks). Choanal microvilli are visible (arrow).

Fig. 19—Detail of a choanocyte, showing phagosomes (ph), and small (sv) and large (lv) secretion vesicles. Arrowheads point to choanal microvilli.

Fig. 20—Enlarged view of a choana (cho) surrounding a flagellum. An unidentified body, probably a tangential section of the choanocyte, lies within the choana (asterisk).

Fig. 21—Detail of an archeocyte, with vesicles (v) and phagosomes (arrows) in its cytoplasm.

Fig. 22—Light microscope image of a section through the tip of a conule, showing the primary supporting fibre (arrow) with mineral inclusions.

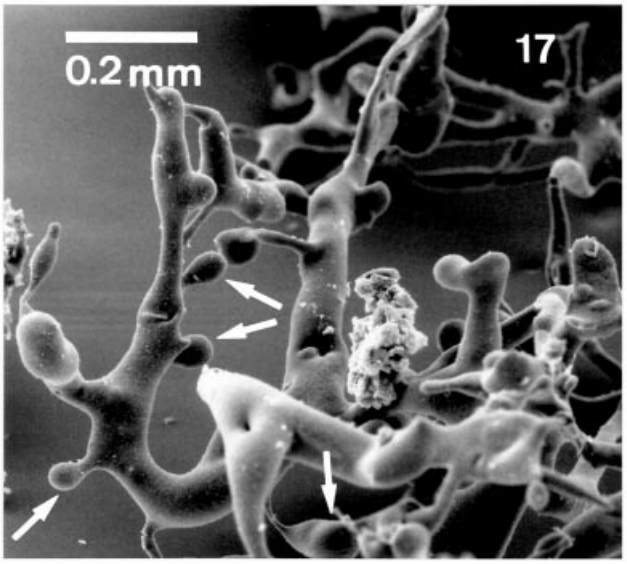

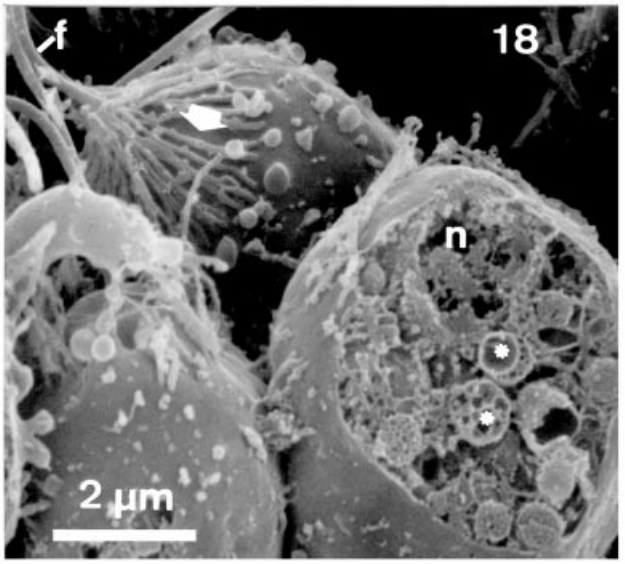

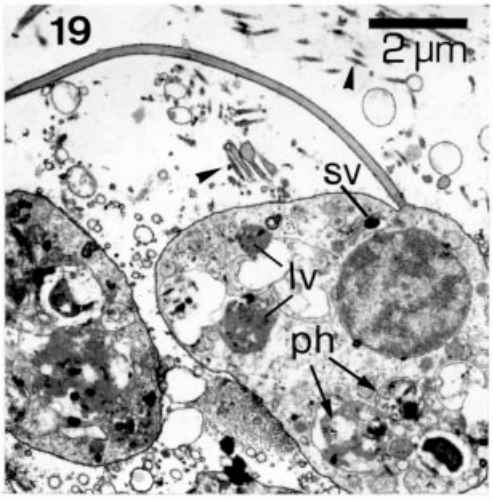

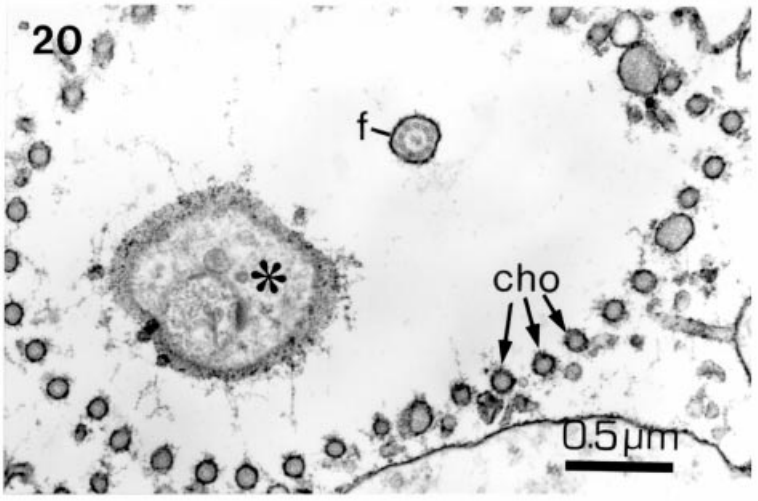

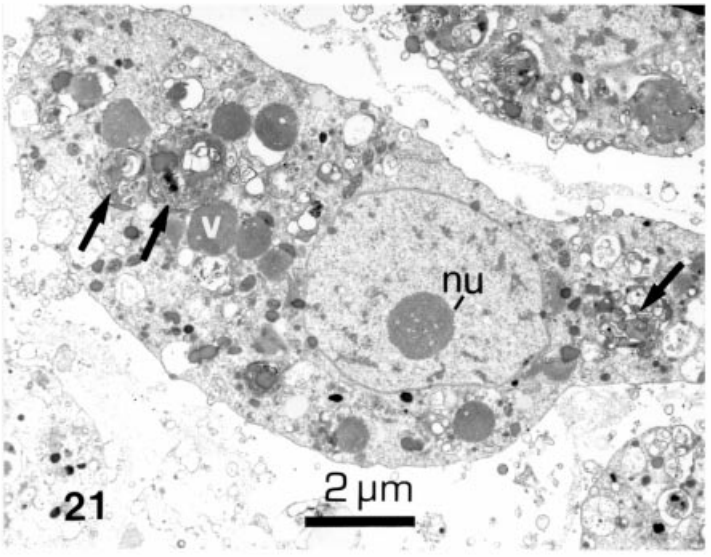

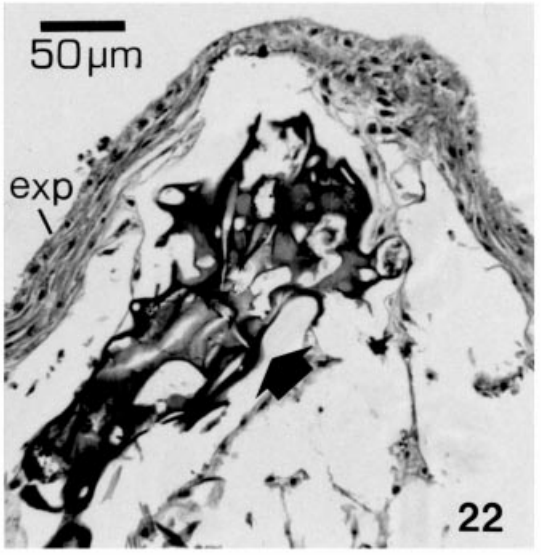

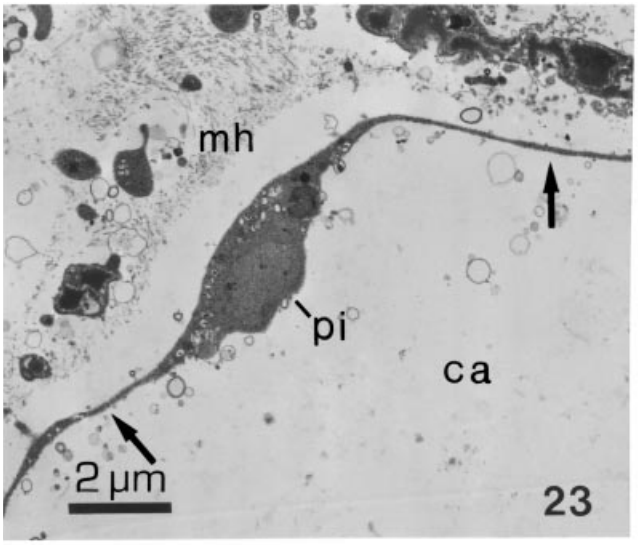

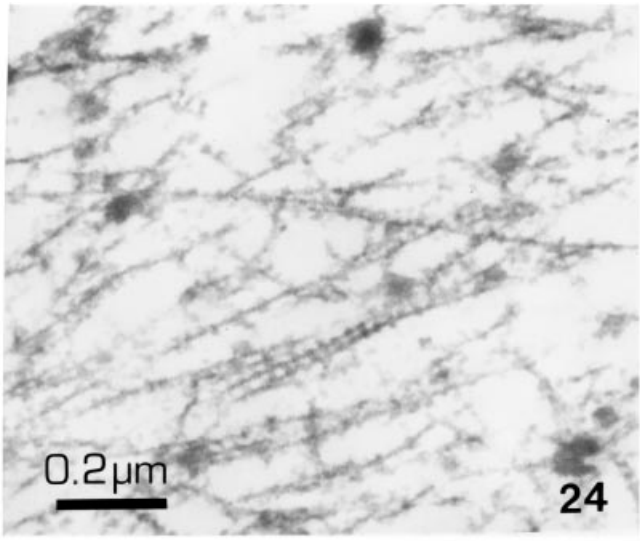

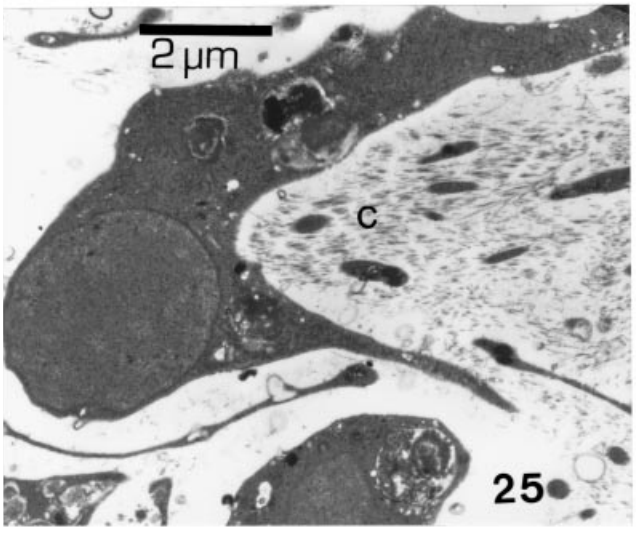

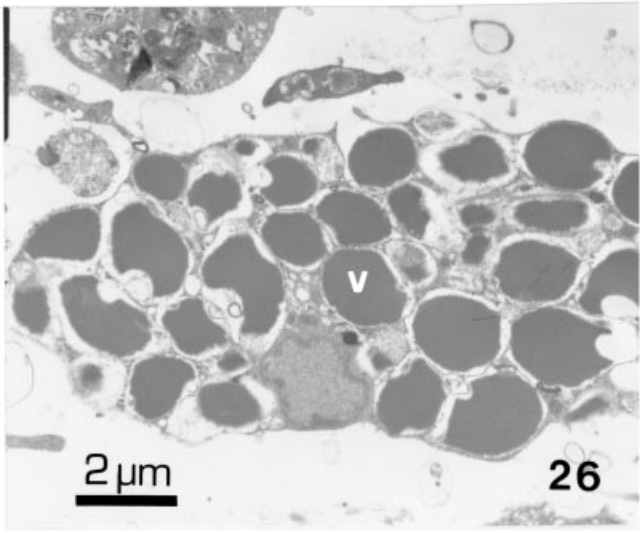

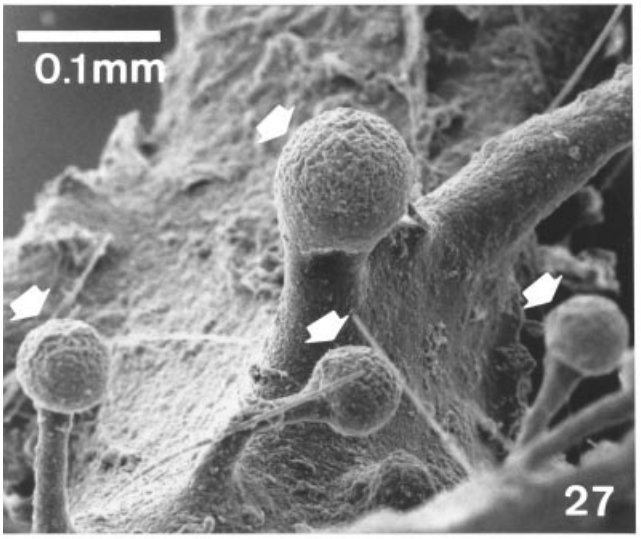

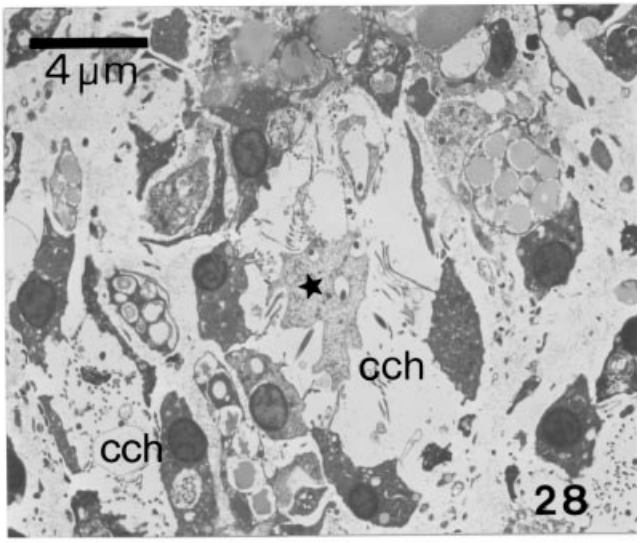

measure up to 20 μm in length, while the thickness in the nucleus region is ≈ 2–4 μm (Fig. 23). The endopinacocytes display a dark, granular aspect due to the many small vesicles and ribosomes, together with a well developed endoplasmatic reticule and a Golgi complex. The exopinacocytes are approximately squared in shape and their nuclei lie in a basal position. A single layer of pinacocytes lines the external surfaces and the internal canals. There are no obvious gaps between pinacocytes although overlapping of contiguous cells is usual.

The mesohyl of the ectosome of *C. crambe* is rich in collagen fibrils and other cellular elements: collencytes and spherulous cells. Collagen (Fig. 24) belongs morphologically to the rough type (Garrone 1985), with 150–200 Å-wide microfibrils, showing a banding at about 200 Å. The collencytes are similar in shape and structure to that described for *D. avara*, except in their much darker cytoplasm (Fig. 25). They have a large nucleolate nucleus and pseudopodia. The spherulous cells are abundant, spherical or ovoid (Fig. 26), with sizes ranging between 10 and 16 μm in diameter, and with a nucleus ≈ 2 μm in diameter. There are two main types of spherulous cells according to the structure and density of the inclusions (spherules). The first type has subspherical inclusions, dense to electrons and uniform in size (Fig. 26). They are bright orange in colour when observed under a light microscope. This cell type is responsible for the red to orange colour exhibited by living sponges and corresponds therefore to the chromocytes described for *Trikentrion* and *Cyamon* species (Smith 1968). The second type of spherulous cells contains colourless, more heterogeneous inclusions. In both cases the spherules are so developed that they force the nucleus into an irregular, star-shaped aspect. These cells are located near the surface or close to the canals.

The aquiferous system features small choanocyte chambers of ≈ 25 μm in diameter in histological sections, although measures obtained with corrosion casts can reach up to 70 μm in diameter, the apopyles measuring ≈ 20 μm in the castings (Fig. 27). The choanosome of *C. crambe* presents a more compact structure than that of *D. avara*, with abundant ground substance (matrix) and a greater diversity of cellular types (Fig. 28). The choanocyte chambers feature between 7 and 13 choanocytes per section. The choanocytes are small, 3–4.5 μm wide and 1.5–3 μm high (Fig. 29). The nuclei are located in the basal zone and they are usually anucleolate. These cells harbour numerous phagosomes and vacuoles. The collar size is 3–4 μm in diameter, the number of microvilli varies between 26 and 37, with a mean diameter of 0.09 μm each, and with a separation between them of 0.08 ± 0.05 μm. Flagella are directed towards the centre of the chamber, and appear intermingled with pseudopodia of the central cell. The latter cell type, which is lacking in *D. avara*, is placed singly in the middle of the choanocyte chambers (Fig. 28). The central cells range in size between 3 and 7 μm in diameter, and exhibit long, narrow and complicated pseudopodia. They belong to the D-type described by Reiswig and Brown (1977).

Archeocytes, collencytes, spherulous cells and sclerocytes are also present in the choanosome. Archeocytes (Fig. 30) have elongated or irregular morphology (up to 7.5–10 μm in length) with a large (up to 5 μm in diameter) nucleolate nucleus, abundant glycogen reserves and a variable number of phagosomes. They are relatively abundant in the mesohyl, sometimes displaying pseudopodia. Collencytes and spherulous cells are similar to those in the ectosome. Sclerocytes (Fig. 31) are 10–12 μm in diameter, with a large nucleolate nucleus, abundant small vacuoles containing clear material and no glycogen formations. Their most conspicuous feature is the large number of mitochondria. They are found in association with developing spicules. These spicules are composed of an axial filament surrounded by silica deposits (Figs 31, 32). The section of a young spicule is triangular, while fully developed spicules have a circular section. The axial filament usually retains the triangular shape, but with rounded angles.

Perispicular spongin and spicules are found both in the choanosome and the ectosome. The spicules can appear isolated in the mesohyl or, more commonly, embedded into spongin. The spongin is surrounded by densely packed collagen fibrils that appear to fuse with it. Flat, pinacocyte-like cells are abundant around the spongin (Fig. 33).

Occasionally, the presence of cell disgregation areas in the ectosome (Fig. 34) and basal zone of the choanosome has been observed. They are always associated with areas rich in degenerating spherulous cells that can be seen in some sections leaving the sponge through both the canals and the outer surface (Figs 4 and 34).

Discussion

Cytological and microarchitectural parameters of sponges have been used for taxonomical purposes (Vacelet *et al.* 1989; Langenbruch and Jones 1990; Boury-Esnault *et al.*

Figs 23–28—*Crambe crambe*. c collagen, ca canal, cch choanocyte chamber, mh mesohyl, pi pinacocyte, v secretion vesicle.
Fig. 23—Image of an endopinacocyte with long lateral processes (arrows).
Fig. 24—Enlarged image of some collagen fibrils.
Fig. 25—Detail of a collencyte with a bundle of collagen fibrils (c).
Fig. 26—View of a spherulous cell whose vesicles (v) contain an electron dense material.
Fig. 27—SEM detail of a corrosion casting showing some choanocyte chambers (arrowed).
Fig. 28—View of the choanosome, showing choanocyte chambers and a mesohyl rich in spherulous cells. A central cell (star) is visible in the lumen of a choanocyte chamber.

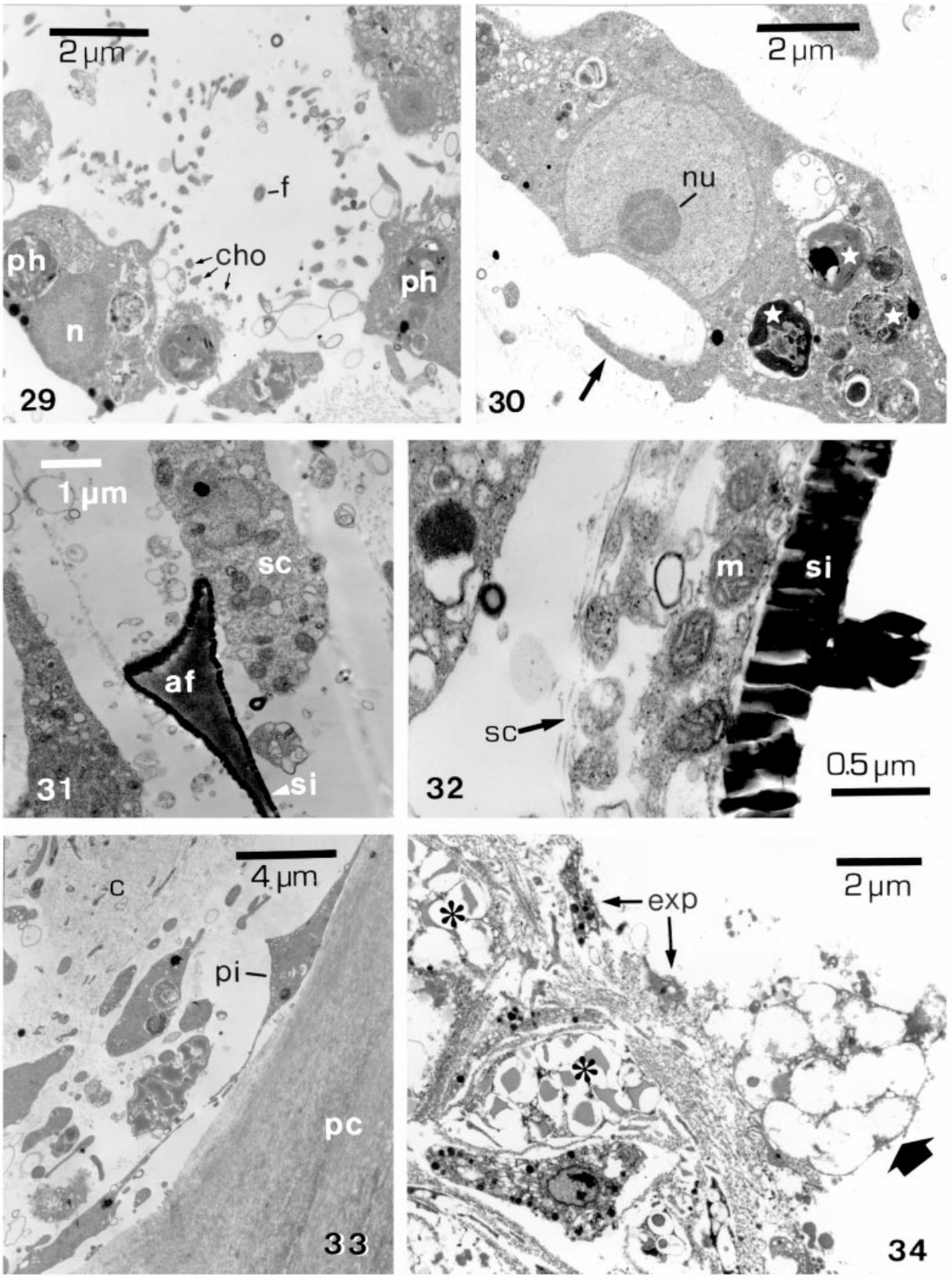

1994; Vacelet and Perez 1998). However, the biological correlates of microarchitectural parameters have not been taken into consideration in studies describing the structure of sponges.

Here we show that cytology and structural parameters may be good descriptors of the general biological strategy of the sponges. Among these parameters are the degree of development of the aquiferous system and the relative investment in supportive (spicules, spongin, intercellular collagen), cellular and matrix material. These parameters have the advantage that they are not only qualitative, but can be quantified and analysed statistically, allowing formal comparisons among species, as well as intraspecific studies of relative allocation of the energy expenditure (Uriz *et al.* 1995). To our knowledge, this is the first instance of a quantitative comparison of microstructural pattern in sponges.

Although both species studied are encrusting, their architecture is clearly distinct. The most conspicuous differences are the thickness, the ectosome/choanosome rate, the higher porosity of *D. avara*, and the amount of matrix (ground substance) in *C. crambe*. Intercellular collagen fibrils are extraordinarily abundant in the ectosome of both species. They are packed parallel to the sponge surface providing structural support and mechanical protection. The collagen/cell rate is higher in the ectosome of *D. avara* than in that of *C. crambe* (mean of 1.3 vs. 0.88, respectively). This is due to the high number of collagen-producing collencytes in the ectosome of *D. avara* and the absence in this species of spherulous cells, which are abundant in the ectosome of *C. crambe*. These spherulous cells possibly play a defensive role in this species (Uriz *et al.* 1996a). On the other hand, both the collagen and the cellular material is less abundant in the choanosome of *C. crambe* than in *D. avara*, and this is due to the noticeable amount of mesohyl free of collagen and cells (matrix) in *C. crambe*. The aquiferous system, corresponding to the lumen of canals and choanocyte chambers, occupies a much higher fraction of *D. avara* than of *C. crambe* sections. This difference led us to calculate the amount of the different materials with respect to both the total section area and the area without porosity. The latter may provide a more standardized measure allowing for between-species comparison. This comparative approach shows that, while differences are not significant for collagen fibrils, both the amount of fibres and cells is higher for *D. avara* when the two sponge layers are combined.

C. crambe has siliceous spicules that accomplish a supportive function and are reinforced by spongin. *D. avara* lacks spicules and is about three times thicker than *C. crambe*. This may explain the much higher investment in spongin fibre production in *D. avara*. Foreign materials also reinforce the fibres of *D. avara*. They comprise spicules, shell debris and sand grains. These materials are captured and transported towards the conules, where they are enclosed in the fibres during their growth (Teragawa 1985). The production of spicules in *C. crambe* probably involves a higher metabolic cost when compared to incorporation of foreign material. This cost is associated with the high metabolic activity of sclerocytes (indeed, this is the cell type richest in mitochondria).

The mean diameter of inhalant pores, the amount of canals and chambers, and the area of the chambers are significantly greater in *D. avara* than in *C. crambe*. These values are consistent with the higher clearance rates reported for the former species (Turon *et al.* 1997). The casting method gave better results when plastic perfusion was made underwater, especially in the case of *D. avara*. In general, choanocyte chamber measures obtained on the castings were bigger than those obtained through histological techniques. This may reflect the known shrinking of structures during histological preparation (Hayat 1981). Plastic perfusion may have caused a distension of chambers, a possibility already noted by Rosell (1996).

At the cytological level, remarkable differences are also found between these species. The diversity of cellular types is higher in *C. crambe*. Spherulous cells, central cells and sclerocytes are not present in *D. avara*. On the other hand, while collencytes and archeocytes present a similar morphology in both species, the choanocytes and pinacocytes are different. Both are greater in *D. avara* and are richer in secretion vesicles and phagosomes. This may be related to their higher phagocytic activity (Turon *et al.* 1997) and also to the chemical defence mechanism of both species. Cellular fractionation has demonstrated that the toxic metabolites of *C. crambe* are stored in the spherulous cells (Uriz *et al.* 1996a), while those of *D. avara* accumulate in the choanocytes (Uriz *et al.* 1996c).

C. crambe is a sponge with abundant matrix substance;

Figs 29–34—*Crambe crambe*. af axial filament, c collagen, cho choana, exp exopinacoderm, f flagellum, m mitochondrion, *n* nucleus, nu nucleolus, pc perispicular collagen, pi pinacocyte, sc sclerocyte, si silica deposit.

Fig. 29—Detail of a choanocyte chamber. Note the phagosomes in the choanocytes and the choana surrounding a flagellum.

Fig. 30—Detail of an archeocyte. The cytoplasm is filled with phagosomes (stars) and a pseudopodium (arrow) is protruding.

Fig. 31—Detail of a sclerocyte and a developing spicule. Only a thin layer of silica has been deposited around the axial filament.

Fig. 32—Enlarged view of the silica layer of a developing spicule and the sclerocyte surrounding it.

Fig. 33—Mass of compact perispicular collagen (spongin) lined by pinacocyte-like cells.

Fig. 34—View of a degenerating area close to the sponge's surface. The exopinacoderm appears disorganized. A residual spherulous cells is about to be shed (arrow) while others (asterisks) appear to be degenerating.

its aquiferous system occupies less than 25% of the sponge section. In addition, it produces a mineral skeleton and an array of chemical defences. Overall, it invests more in structure than in cellular components (S/C ratio of 1.188). *C. crambe* produces more than double structural elements per cell area than *D. avara*. These features point to a species that is slow growing and is able to maintain the space acquired in the face of other competitors. The known biological parameters of *C. crambe* are in agreement with these microstructural features: *C. crambe* grows very slowly (average monthly growth rate of small sponges during a two-year period of 0.03 ± 0.01, Turon *et al.* 1998). It is well-defended chemically and is a good space competitor (Becerro *et al.* 1997). On the other hand, *D. avara* has most of its sponge section occupied by the canals and chambers of the aquiferous system with little matrix material and, among the cellular types, those able to ingest food particles (choanocytes and pinacocytes) largely predominate. *D. avara* produces twice as much cellular material as structural material (S/C ratio of 0.455). These features suggest that this species can grow at high rates and a more opportunistic strategy of space acquisition and maintenance. Again, the existing evidence is coherent with the structural results: *D. avara* has a strong filtering activity (Ribes 1998), it is susceptible to predation (Uriz *et al.* 1996b), and it features a dynamic growth pattern with alternating phases of active growth and retraction (average monthly growth rate for small sponges during a two-year period of 0.1 ± 0.02, authors' unpublished res.).

Our study shows that there is a wide range of microarchitectural patterns, even in species of a similar growth form, and that these patterns appear to be correlated with biological strategies. Of course, some of these features may be evolutionarily constrained (we are studying sponges of different Orders) instead of life history driven. In this sense, cytological parameters (e.g. presence or absence of some cell types) are, in our opinion, more prone to be phylogenetically determined than structural parameters such as thickness, investment in supportive material, etc. The latter are more susceptible to vary as an adaptation to environmental conditions and hence correlate with life history traits (e.g. spicule production, which has strong architectural implications, can be limited by environmental conditions Maldonado *et al.* 1999). Indeed, sponges are known for their extreme morphological plasticity. Our comparison can be considered as a first step towards understanding the relationship between structure and biology in sponges. As more species are investigated from this perspective, structural characters may prove to be useful descriptors of biological features in sponges.

Acknowledgements

The Scientific and Technical Services of the University of Barcelona provided electron microscope and image analysis facilities, as well as technical support. This research was supported by projects DGCYT PB94–0015 and CICYT MAR95–1764 of the Spanish Government and 1995SGR 00443 of the Catalan Government.

References

Bavestrello, G., Burlando, B. and Sarà, M. 1988. The architecture of the chanal system of *Petrosia ficiformis* and *Chondrosia reniformis* studied by corrosion casts (Porifera, Demospongiae). – *Zoomorphology* **108**: 161–166.

Becerro, M. A., Uriz, M. J. and Turon, X. 1997. Chemically-mediated interactions in benthic organisms: the chemical ecology of *Crambe crambe* (Porifera, Poecilosclerida). – *Hydrobiologia* **356**: 77–89.

Boury-Esnault, N., Hajdu, E., Klautau, M., Custodio, M. and Borojevic, R. 1994. The value of cytological criteria in distinguishing sponges at the species level: the example of the genus Polymastia. – *Canadian Journal of Zoology* **72**: 795–804.

Burlando, B., Bavestrello, G., Sarà, M. and Cocito, S. 1990. The aquiferous system of *Spongia officinalis* and *Cliona viridis* (Porifera) based on corrosion casts analysis. – *Bolletino Di Zoologia* **57**: 233–239.

Buss, L. W. 1979. Habitat selection, directional growth and spatial refuges: why colonial animals have more hiding places. In: Larwood, G. and Rosen, B. R. (Eds): *Biology and Systematics of Colonial Organisms*, pp. 459–497. Academic Press, New York.

Crispino, A., De Giulio, A., De Rosa, S. and Strazzullo, G. 1989. A new bioactive derivative of avarol from the marine sponge *Dysidea avara*. – *Journal of Natural Products* **52**(3): 646–648.

De Giulio, A., De Rosa, S., Di Vincenzo, G. and Strazzullo, G. 1990. Further bioactive derivative of avarol from *Dysidea avara*. – *Tetrahedron* **46**(23): 7971–7976.

De Vos, L., Rützler, K., Boury-Esnault, N., Donadey, C. and Vacelet, J. 1991. – *Atlas of Sponge Morphology*. Smithsonian Institution Press, Washington.

Diaz, J. P. 1979. Variations, differentiations et fonctions des categories cellulaires de la demosponge d'eau saumâtre *Suberites nana* Nardo au cours du cycle biologique annuel et dans des conditions experimentales. Ph D Thesis. University of Sci. Technical Languedoc.

Garrone, R. 1985. The collagen of the Porifera. In: Bairati, A. and Garrone, R. (Eds): *Biology of Invertebrate and Lower Vertebrate Collagens. NATO ASI Series A: Life Sciences 93*, pp. 157–175. Plenum Press, New York.

Gross, J., Sokal, Z. and Rougvie, M. 1956. Structural and chemical studies on the connective tisssue of marine sponges. – *Journal of Histochemistry and Cytochemistry* **4**: 227–246.

Hayat, M. A. 1981. *Fixation for Electron Microcopy*. Academic Press Inc, New York.

Jackson, J. B. C. 1979. Morphological strategies of sessile animals. In: Larwood, G. and Rosen, B. R. (Eds): *Biology and Systematics of Colonial Organisms*, pp. 499–555. Academic Press, New York.

Johnson, I. S. and Hildemann, W. H. 1982. Cellular organization in the marine Demosponge *Callyspongia diffusa*. – *Marine Biology* **67**: 1–7.

Langenbruch, P. F. and Jones, W. C. 1990. Body structure of marine sponges. VI. Choanocyte chamber structure in the Haplosclerida (Porifera, Demospongiae) and its relevance to the phylogenesis of the group. – *Journal of Morphology* **204**: 1–8.

Maldonado, M., Carmona, M. C., Uriz, M. J. and Cruzado, A. 1999. Decline in Mesozoic reef-building sponges explained by silicon limitation. – *Nature* **401**: 785–788.

Martoja, R. and Martoja, M. 1970. – *Técnicas de Histología Animal*. Toray Masson, Barcelona.

Minale, L., Riccio, R. and Sodano, G. 1974. Avarol, a novel sesquiterpenoid hydroquinone with a rearranged drimane skeleton from the sponge *Dysidea avara*. – *Tetrahedron Letters* **38**: 3401–3404.

Müller, W. E. G., Zahn, R. K., Gasic, M. J., Dogovic, N., Maidhof, A., Becker, C., Diehl-Seifert, B. and Eich, E. 1985. Avarol, a cytostatically active compound from the marine sponge *Dysidea avara*. – *Comparative Biochemistry and Physiology* **80**: 47–52.

Reiswig, H. and Brown, M. 1977. The central cell of sponges. – *Zoomorphology* **88**: 81–94.

Ribes, M. 1998. Feeding activity and diet of benthic suspension-feeders related to metabolic requirements and seston composition. Ph D Thesis. University of Barcelona.

Rosell, D. 1996. Systematics, biology and ecology of the Mediterranean excavating sponges. Ph D Thesis. University of Barcelona.

Sica, D., Piccialli, V. and Pronzato, R. 1987. D 5,7 sterols from the sponges *Ircinia pipetta* and *Dysidea avara*. Identification of cholesta-5,7,24-trien-3B-OL. – *Comparative Biochemistry and Physiology* **88**: 293–296.

Simpson, T. L. 1984. *The Cell Biology of Sponges*. Springer-Verlag, New York.

Smith, V. E. 1968. Comparative cytology and biochemistry of two marine sponges. Ph D Thesis, University of California, San Diego.

Teragawa, C. K. 1985. Mechanical function and regulation of the skeletal network in *Dysidea*. – *3rd International Sponge Conferences*, 252–258.

Turon, X., Galera, J. and Uriz, M. J. 1997. Clearance rates and aquiferous systems in two sponges with contrasting life-history strategies. – *Journal of Experimental Zoology* **278**: 22–36.

Turon, X., Tarjuelo, I. and Uriz, M. J. 1998. Growth dynamics and mortality of the encrusting sponge *Crambe crambe* (Poecilosclerida) in contrasting habitats: correlation with population structure and investment in defence. – *Functional Ecology* **12**: 631–639.

Uriz, M. J., Turon, X., Becerro, M. A., Galera, J. and Lozano, J. 1995. Patterns of resource allocation to somatic, defensive and reproductive functions in the Mediterranean encrusting sponge *Crambe crambe* (Demospongiae, Poecilosclerida). – *Marine Ecology Progress Series* **124**: 159–170.

Uriz, M. J., Becerro, M. A., Tur, J. M. and Turon, X. 1996a. Location of toxicity within the Mediterranean sponge *Crambe crambe* (Demospongiae: Poecilosclerida). – *Marine Biology* **124**: 583–590.

Uriz, M. J., Turon, X., Becerro, M. A. and Galera, J. 1996b. Feeding deterrence in sponges. The role of toxicity, physical defenses, energetic contents, and life-history stage. – *Journal of Experimental Marine Biology and Ecology* **205**: 187–204.

Uriz, M. J., Turon, X., Galera, J. and Tur, J. M. 1996c. New light on the cell location of avarol within the sponge *Dysidea avara* (Dendroceratrida). – *Cell and Tissue Research* **285**: 519–527.

Vacelet, J., Boury-Esnault, N., De Vos, L. and Donadey, C. 1989. Comparative study of the choanosome of Porifera. II. The Keratose sponges. – *Journal of Morphology* **201**: 119–129.

Vacelet, J. and Perez, T. 1998. Two new genera and species of sponges (Porifera, Demospongiae) without skeleton from a Mediterranean cave. – *Zoosystema* **20**: 5–22.

